Quantitative Analysis and Molecular Docking Simulation of Flavonols from Eruca sativa Mill. And Their Effect on Skin Barrier Function

Jihye Park , Wonchul Choi , Jayoung Kim , Hye Won Kim , Jee-Young Lee , Jongsung Lee * , Bora Kim *

Posted Date: 29 November 2023

doi: 10.20944/preprints202311.1891.v1

Keywords: Eruca sativa; Skin barrier function; Peroxisome proliferator activated receptor-α; Anti-inflammation; Docking simulation

Article

Quantitative Analysis and Molecular Docking Simulation of Flavonols from *Eruca sativa* Mill. and Their Effect on Skin Barrier Function

Jihye Park [1,*], Wonchul Choi [2,*], Jayoung Kim [1], Hye Won Kim [1], Jee-Young Lee [3], Jongsung Lee [2,] and Bora Kim [1,4 **]**

[1] Department of Chemistry, The Graduate School of Mokwon University Daejeon, South Korea; rmarkd545@naver.com (J. P.); kjo08@naver.com (J. K.); kxxhxxwxx98@naver.com (H. W. K.); bora0507@mokwon.ac.kr (B. K)

[2] Interdisciplinary Program in Biocosmetics, Sungkyunkwan University, Suwon, South Korea; wonchulc@g.skku.edu (W. C.); bioneer@skku.edu (J. L.)

[3] Structure Based Drug Design Laboratory, New Drug Development Center, Daegu Gyeongbuk Medical Innovation Foundation (K-Medi hub), Daegu, South Korea; jyoung@kmedihub.re.kr (J. L.)

[4] Department of Cosmetics Engineering, Mokwon University, Daejeon, South Korea; bora0507@mokwon.ac.kr

* Correspondence: bora0507@mokwon.ac.kr

Abstract: *Eruca sativa* is a commonly used edible plant in Italian cuisine. E. sativa 70% ethanol extract (ES) was fractionated with five organic solvents. Ethyl acetate fraction(EEA) had the highest antioxidant activity, which was correlated with the total polyphenol and flavonoid content. ES and EEA acted as PPAR-α ligands by PPAR-α competitive binding assay. EEA significantly increased cornified envelope formation as a keratinocyte terminal differentiation marker in HaCaT cells. Further, it significantly reduced nitric oxide and pro-inflammatory cytokines in lipopolysaccharide-stimulated RAW 264.7 cells. The main flavonol forms detected in high amounts from EEA are mono-, and di-glycoside of each aglycone. Flavonol mono-glycosides were shown to be a potent PPAR-α ligand using molecular docking simulation and showed the inhibition of nitric oxide. These results suggest that *E. sativa* is suitable for use in improving skin barrier function and inflammation in skin disorders, such as atopic dermatitis.

Keywords: *Eruca sativa*; skin barrier function; peroxisome proliferator activated receptor-α; anti-inflammation; docking simulation

1. Introduction

The skin is the outermost organ that protects against ultraviolet radiation, environmental pollutants, harmful microbes, and dry environments. Most of the protective function is provided by the epidermis, with various layers including the stratum corneum (SC), stratum granulosum, stratum spinosum, and stratum basale [1]. The SC of terminally differentiated cornified cells is the outermost epidermis, which forms the barrier properties of the skin [2]. Atopic dermatitis (AD), a skin barrier disease, is a chronic inflammatory skin disorder characterized by eczematous and pruritic skin. Enormous changes in the composition and function of the epidermal barrier influence the initiation and maintenance of skin inflammation in AD [3].

Peroxisome proliferator-activated receptors (PPARs) are ligand-activated transcription factors belonging to the nuclear receptor family. PPAR-α is highly expressed in many tissues, including the heart, kidney, liver, skeletal muscle, and epidermis, where it is an important regulator of lipid metabolism [4]. Topical treatment with PPAR-α agonists was found to restore epidermal homeostasis in skin barrier disruption models [5]. The PPAR-α agonists, WY14643 and ciglitazone, elevated the expression of cornified envelope (CE)-associated proteins [6]. Therefore, screening for new agonists is required to determine whether activators of PPAR-α can improve keratinocyte

Preprints (www.preprints.org) | NOT PEER-REVIEWED | Posted: 29 November 2023 doi:10.20944/preprints202311.1891.v1

differentiation. Topical treatment with a PPAR-α activator showed potent anti-inflammatory effects in an AD model, which was associated with the alleviation of the pro-inflammatory cytokines, viz. TNF-α and IL-6 [7,8]. Therefore, activating PPAR-◎ and anti-inflammatory activities can improve skin barrier function.

Eruca sativa Mill. is an edible annual plant that inhabits the Mediterranean coast, is referred to as rocket or arugula, and is commonly used in Italian foods [9]. *E. sativa* is known to have anti-inflammatory activity through inhibiting the skin barrier improvement effect and inflammatory cytokines. Further, it contains various phytochemicals, thus its antioxidant, anti-microbial, and PPAR-α agonistic activities [10–13]. We previously reported that *E. sativa* crude extract has various functions in improving the skin barrier [8]. In this study, we aimed to determine the skin barrier improvement and anti-inflammatory effect of each organic solvent fraction of *E. sativa* and examine whether the major flavonols identified by instrumental analysis and *in silico* molecular docking simulation are PPAR-α ligands

2. Results and discussion

2.1. Antioxidant activity

Antioxidant activity was investigated through the DPPH radical scavenging and ROS detection assays using H_2DCFDA in LPS-stimulated RAW264.7 macrophages. EEA and EBuOH showed the highest radical scavenging activities compared to the other fractions. The DPPH scavenging activities of the fractions in decreasing order were as follows: EEA > EBuOH > ES > ECHCl3 > EDW > EHEX (Table 1). The intracellular ROS scavenging activity, which was monitored by dichlorofluorescein (DCF) fluorescence intensity, was increased by LPS-induced oxidative stress in EEA. The green fluorescence intensity was proportional to the ROS levels within the cell cytosol. Further, EEA 50, 100 μg/mL showed a dose-dependent antioxidant effect (Figure 1a).

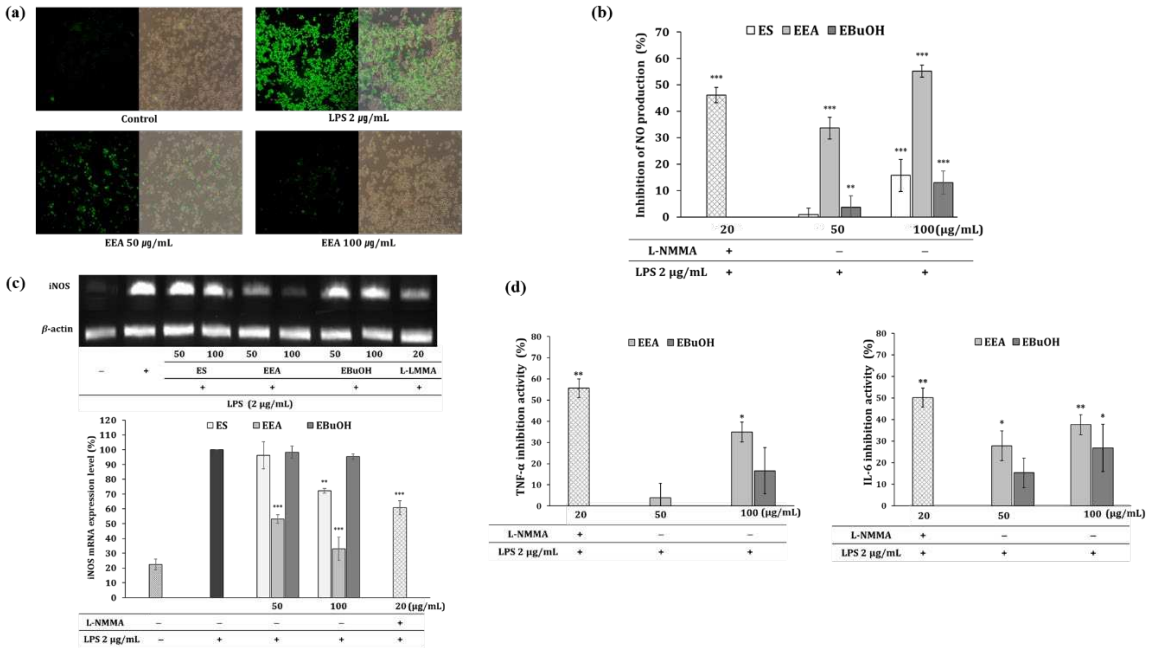

Figure 1. (a) Fluorescence microscopic image of cellular ROS in LPS-induced RAW 264.7 cells with EEA treatment. The intracellular ROS scavenging activity, which was monitored by dichlorofluorescein (DCF) fluorescence intensity, was increased by LPS-induced anti-oxidative stress in EEA 50, 100 μg/mL. (b) Inhibition of NO production. (c) Inhibition of iNOS mRNA expression. Effect of EEA and EBuOH on inflammatory cytokines. (d) Inhibition of inflammatory cytokines TNF-α, IL-6. by ELISA. Values are presented as the mean±SD of triplicate measurements (*p<0.05, **p<0.01, ***p<0.001, compared with negative control).

Preprints (www.preprints.org) | NOT PEER-REVIEWED | Posted: 29 November 2023 doi:10.20944/preprints202311.1891.v1

Table 1. Table 1. DPPH radical scavenging activity, total polyphenol contents and total flavonoid contents of *E. sativa* fractions.

Sample	SC_{50} (μg/mL)	GAE (mg/g)	QE (mg/g)
ES	610.40	32.22±2.70	38.46±15.55
EEA	229.38 ***	104.99±5.88 ***	74.24±1.67 **
EBuOH	494.93 **	88.42±2.17 ***	53.41±0.33
$ECHCl_3$	650.19	44.35±3.55	39.30±8.29
EDW	1993.50	16.58±0.89	27.43±8.18
EHEX	2078.39	8.52±1.00	44.73±14.31
L-ascorbic acid	23.86 ***	-	-

2.2. Determination of total phenolic and flavonoid content

Phenolic compounds are synthesized by plants in response to various stresses such as infection, injury, and UV radiation [15]. Flavonoids belong to the polyphenol subgroup with various health-improving effects [16]. Quantification of total phenolic content (TPC) and total flavonoid content (TFC) using calibration curves of gallic acid and quercetin, respectively, showed the greatest abundance in EEA (104.99 ± 5.88 mg GAE/g extract, 74.24 ± 1.67 mg QE/g extract) followed by EBuOH (88.42 ± 2.17 mg GAE/g extract, 53.41 ± 0.33 mg QE/g extract) as summarized in Table 1. These results indicate that EEA and EBuOH contained high flavonoid contents compared to TPC. As such, the most antioxidative fraction was highly correlated with total polyphenol and flavonoid contents.

2.3. Anti-inflammatory effects

The activation of macrophages by the bacterial surface molecule LPS leads to the production of ROS and NO radicals, which play important roles in inflammation [17]. ES, EEA, and EBuOH showed cell viability of more than 80% in RAW 264.7 cells at concentrations < 100 μg/mL. Treatment of the cells with 100 μg/mL of ES, EEA, and EBuOH significantly inhibited NO production, which is a well-known inflammatory mediator in LPS induced RAW 264.7 cells (Figure 1b). Treatment with 100 μg/mL EEA significantly also reduced iNOS mRNA expression (Figure 1c). In addition, 100 μg/mL EEA and EBuOH significantly inhibited pro-inflammatory cytokines production such as IL-6 and TNF-α (Figure 1d). Three major flavonol aglycones and their mono glucosides (quercetin, kaempferol, isorhamnetin quercetin 3-glucoside, kaempferol 3-glucoside, isorhamnetin 3-glucoside) which were were confirmed to inhibit NO production (Table 2), quantified in EEA (Table 3). Quercetin 3-glucoside showed the strongest anti-inflammatory effect (IC50 = 1.81 μM). The anti-inflammatory effect of this fraction was postulated to be a complex synergistic effect of three major flavonol aglycones and their mono glucosides, as the anti-inflammatory effect was better than that of other fractions [18].

Table 2. The inhibition of NO production of flavonols.

Sample	IC_{50} (μM)
Quercetin-3-glucoside	1.81
Kaempferol-3-glucoside	58.33
Isorhamnetin-3-glucoside	-
Quercetin	72.27
Kaempferol	89.38
Isorhamnetin	442.02

Preprints (www.preprints.org) | NOT PEER-REVIEWED | Posted: 29 November 2023 doi:10.20944/preprints202311.1891.v1

Table 3. Identification of flavonols of each fraction by LC/MS data based on MS2 fragmentation pattern.

No.	T_R(min)	Formula	Ion	Experimental m/z	Calculated m/z	Fragment	Identification
1	6.2	$C_{27}H_{30}O_{17}$	[M-H]-	625.25	625.14	463, 301	Quercetin 3,4'-diglucoside
2	6.9	$C_{27}H_{30}O_{16}$	[M-H]-	609.25	609.15	477, 315	Kaempferol 3,4'-diglucoside*
3	7.9	$C_{28}H_{32}O_{17}$	[M-H]-	639.25	639.16	447, 285	Isorhamnetin 3,4'-diglucoside*
4	11.4	$C_{21}H_{20}O_{12}$	[M-H]-	463.17	463.09	301	Quercetin-3-glucoside
5	14.6	$C_{21}H_{20}O_{11}$	[M-H]-	447.17	447.09	284, 255, 327	Kaempferol 3-glucoside
6	15.4	$C_{22}H_{22}O_{12}$	[M-H]-	477.17	477.10	314, 357, 285	Isorhamnetin 3-glucoside
7	25.1	$C_{15}H_{10}O_7$	[M-H]-	301.08	301.03	179, 151, 273	Quercetin
8	32.6	$C_{15}H_{10}O_6$	[M-H]-	285.08	285.03	151, 257, 229, 185	Kaempferol
9	33.9	$C_{16}H_{12}O_7$	[M-H]-	315.07	315.05	300	Isorhamnetin

* The identification was checked by the previous study on *E. sativa* referred to Reference [9].

2.4. CE formation and PPAR-α binding assay

To investigate the effects of EEA and ES on keratinocyte differentiation, we measured CE formation as a terminal differentiation marker in HaCaT cells at the low calcium concentration (0.09 mM) [19,20]. When cells were treated with ES and EEA, the CE formation assay was performed at a concentration that resulted in more than 80% cell viability. CE formation was increased by approximately 20–30% following ES and EEA treatments compared to low calcium treatment (Figure 2a). PPARα is a ligand-activated transcription factor that plays an important role in epidermal homeostasis. In a nuclear receptor binding assay based on TR-FRET, EEA and ES competitively replaced the binding of labeled PPAR-α ligands by approximately 18–47% (Figure 2b) [21]. ES and EEA may play a role in activating PPAR-◎ and promoting keratinocyte differentiation for skin barrier recovery [19].

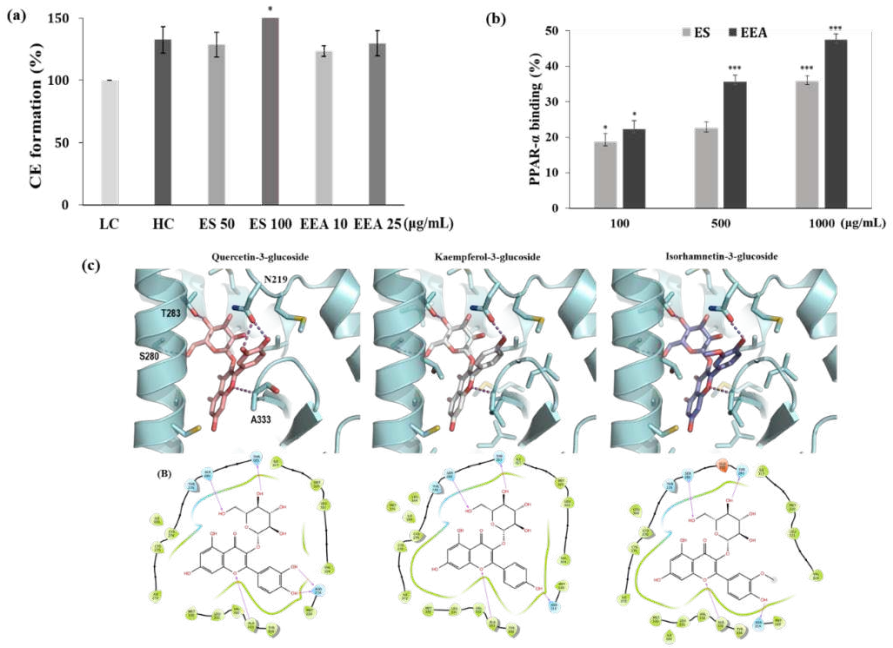

Figure 2. (a) HaCaT Cell viability was determined by WST assay (d) HaCaT cells were cultured in the presence of ES and EEA under low Ca2+ (LC, 0.09 mM) or high Ca2+ (HC, 3.5 mM) treatment. (b) PPAR-α binding activity (c) Analysis of interactions between PPAR-α and three flavonol mono-

 doi:10.20944/preprints202311.1891.v1

glycoside. Ligand interaction diagram supported from docking results. Values are presented as the mean±SD of triplicate measurements (*p<0.05, **p<0.01, ***p<0.001, compared with negative control).

2.5. Binding model prediction between PPAR-α and flavonols

In this study, the initial binding model was determined by rigid docking, and the MM-GBSA calculation, which induces structural changes in the protein according to the binding of the ligand, was used to determine the final binding structure. MM-GBSA are widely used to estimate the binding free energy of small molecules and proteins [22,23]. It is well known that PPAR activators bind to ligand binding domain (LBD) of PPARs and many of PAPR-activator complex structures are elucidated by X-ray crystallography. Quercetin-3-glucoside, a possible activator of PPAR-α, is capable of binding to PPAR-α LBD with low binding energy. The important key interactions of quercetin-3-glucoside are five hydrogen bonds (H-bonds) with PPAR-α residues. The two hydroxyl moieties on the sugar ring formed H-bonds with the side chains of S280 and T283. The other two hydroxyl groups of the B ring also participated in a H-bond interaction with N219. Further, an oxygen atom on the A-ring formed a H-bond with the NH backbone of the A333 residue. H-bond interactions are important in determining whether a ligand binds to a target protein [24]. Five H-bonding interactions between PPAR-α and quercetin-3-glucoside played a role in stabilizing the interaction and increasing binding affinity (Figure 2c). Kaempferol-3-glucoside and isorhamnetin-3-glucoside, also well fitted to activator binding site on PPAR-α and the binding model are like that quercetin-3-glucoside. Quercetin-3-glucoside has two hydroxyls on 3'-, 4-position of B-ring, but the rest flavonols only one hydroxyl moiety at 4'-positon. The absence of hydroxyl moiety on 3'-position of B-ring reduced number of H-bonding interactions than quercetin-3-glucoside. This leads to a diminishing of the binding affinity. The binding free energies resulting from MM-GBSA calculation support that quercetin-3-glucoside has a slightly higher affinity than other two flavonols. These results suggest that quercetin-3-glucoside can more strongly bind to PPAR-α and may act as an activator of PPAR-α.

2.6. Analysis of flavonols

The identification of the major flavonols of each fraction were performed on HPLC-UV-MS. Based on the retention times, molecular formula, MS2 data, reference standards and previous study [25], 9 major compounds were identified, which include: quercetin, kaempferol, isorhamnetin and glucose derivatives of these three aglycones as shown in Table 3. The flavonol content of the crude ethanolic extract of E. sativa and solvent partitioning fractions were quantitated as shown in Table 4. The flavonol composition of the solvent fractions of E. sativa was determined for the first time. Three main flavonol aglycones such as kaempferol, quercetin, and isorhamnetin were detected in EEA with comparatively small amount, which is consistent with our previous results [8]. The main flavonol form of EEA is mono-glycoside of each aglycone detected and the most abundant flavonol mono-glycoside is kaempferol 3-glucoside, 7.4% followed by quercetin-3-glucoside 2.3% and isorhamnetin 3-glucoside 1.4%. The second abundant flavonol form of EEA is the di-glycoside of each aglycone detected such as kaempferol 3,4'-diglucoside, quercetin 3,4'-diglucoside and isorhamnetin 3,4'-diglucoside. On the other hand, the most abundant flavonols form in EBuOH are di-glycoside of the three aglycones, different from that of EEA. Kaempferol 3,4'-diglucoside is the most abundant flavonol in EBuOH fraction because of the higher polarity of n-butanol than that of ethyl acetate. Flavonol di-glycosides are main components in EBuOH, EDW and crude 70% ethanol extract, which is consistent with the study in the past [26–28]. Total flavonol content is comparatively large in EEA (13.2%) and EBuOH (7.7%), which is positively related to the results of the total phenolic and flavonoid content as shown in Table 1. These results also make it possible to study the correlation between chemicals and biological activity. Furthermore, the biological activity of flavonols can be influenced by their steric hindrances at the active site, resulting in the better biological activity of EEA fraction enriched with flavonol mono-glycosides than that of other fractions enriched with flavonol di-glycosides.

 doi:10.20944/preprints202311.1891.v1

Table 4. Flavonols content of each fraction of *E. sativa* by HPLC-UV (% based on each fraction).

flavonols detected	crude extract (by 70%EtOH)	hexane fraction	$CHCl_3$ fraction	ethyl acetate fraction	butanol fraction
Quercetin 3,4'-diglucoside	0.062±0.002	0.049±0.004	N.D.	0.25±0.02	1.05±0.009
Kaempferol 3,4'-diglucoside	0.22±0.006	0.19±0.002	0.010±0.0009	1.26±0.05	5.70±0.05
Isorhamnetin 3,4'-diglucoside	0.048±0.003	0.020±0.002	N.D.	0.12±0.004	0.37±0.02
Quercetin 3-glucoside	0.0055±0.0003	0.0045±0.0003	0.0021±0.0002	2.27±0.07	0.20±0.003
Kaempferol 3-glucoside	0.018±0.0004	0.016±0.0007	N.D.	7.37±0.3	0.31±0.004
Isorhamnetin 3-glucoside	0.0072±0.0003	0.0031±0.0001	N.D.	1.44±0.08	0.099±0.001
Quercetin	N.D.	N.D.	0.0016±0.00007	0.093±0.008	0.0014±0.00009
Kaempferol	0.00071±0.00004	N.D.	0.0042±0.0002	0.32±0.02	N.D.
Isorhamnetin	N.D.	N.D.	0.010±0.0005	0.13±0.006	N.D.
Sum	0.36	0.28	0.03	13.2	7.7

3. Materials and Methods

3.1. Chemicals and reagents

Sigma-Aldrich provided 2,2-diphenyl-1-picrylhydrazyl (DPPH), 2',7'-dichlorofluorescein diacetate (DCF-DA), lipopolysaccharide (LPS), Folin–Ciocalteu (F–C) reagent, gallic acid, AlCl3, Griess reagent, NG-Methyl-L-arginine acetate salt (L-NMMA), WY14643, CaCl2, and HPLC grade standards of quercetin, kaempferol, isorhamnetin, kaempferol 3-glucoside, isorhamnetin 3-glucoside, quercetin 3-glucoside, and quercetin 3,4'-diglucoside. Solvents for extraction and fractionation (ethanol, n-hexane, chloroform, ethyl acetate and n-butanol) and formic acid were purchased from Daejung chemicals & metals (Siheung, Korea). Solvents for LC/MS (methanol, acetonitrile) were purchased from Honeywell Burdick & Jackson (Muskegon, MI, USA).

3.2. Extraction and fractionation of E. sativa

E. sativa leaves were purchased from the Garak agricultural and marine product wholesale market (Garak-dong, Seoul, Korea). After washing with purified water, they were chopped and dried for 24 h at 50 ℃. Next, the leaves (800 g) were refluxed twice and extracted with 5 L of 70% ethanol for 24 h at 55 ℃. The *E. sativa* extract was then filtered through a No.6 filter paper and vacuum evaporated (Advantec, Tokyo, Japan). Lastly, the crude ethanolic extract of *E. sativa* (230 g) was fractionated by the solvent partitioning method (800 ml of each step, 3 times) using its aqueous suspension with the increase of the polarity of the solvent from hexane to n-butyl alcohol. Each fraction was: n-hexane fraction (EHex, 9.6g); chloroform fraction (ECHCl3, 0.4g); ethyl acetate fraction (EEA, 4.5g); n-butyl alcohol fraction (EBuOH, 9.6g); water fraction (EDW, 209.5g).

3.3. Antioxidant activity of 2,2-diphenyl-1-picrylhydrazyl

0.2 mM DPPH solution was used to determine the antioxidant capacity of the extracts, and the reaction was carried out for 30 min in an incubator maintained at 25 ℃. Lower SC50 values (the concentration of each sample for scavenging 50% of radicals) indicated a higher radical scavenging potential. L-Ascorbic acid was used as the positive control.

3.4. Total polyphenol and flavonoid content assay

The total polyphenol content of the extract and its fractions was determined using the Folin–Ciocalteu (F–C) reagent. The samples were mixed with F–C reagent and 700 mM sodium carbonate. After the mixture had reacted for 30 min in an incubator maintained at 25 ℃, absorbance was measured at 765 nm using a microplate reader. The total polyphenol content was expressed in gallic acid equivalent (GAE) mg/g of the extract and each fraction. The total flavonoid content of the extract

 doi:10.20944/preprints202311.1891.v1

and each fraction was determined using a modified aluminum chloride colorimetric method. 5% NaNO2 was added to the sample and reacted followed by mixing with 10% AlCl3. Lastly, the reaction was performed with 1N NaOH at 25 ℃, and the absorbance was measured at 510 nm using a microplate reader. The total flavonoid content was expressed as mg of quercetin equivalent (QE)/g of extract and each fraction.

3.5. Cell culture

Cell lines were purchased from the Korea Cell Line Bank (KCLB, Seoul, Korea). RAW 264.7 and HaCaT cells were cultured in Dulbecco's modified Eagle's medium (DMEM, Welgene, Korea) containing 10% fetal bovine serum (FBS, Gibco) and 1% penicillin-streptomycin (Gibco). Cytotoxicity was determined using a water-soluble tetrazolium salt-1 (WST-1) assay (Dogenbio, Seoul, Korea).

3.6. Cornified envelope formation

HaCaT cells were seeded at a density of 5×105 cells in 60-mm dishes. Cells kept in medium containing 0.09 mM Ca^{2+} (low calcium, LC) were considered undifferentiated. Cells kept in medium containing 3.5 mM Ca^{2+} (high calcium, HC) were used as a positive control to represent the differentiated status. After incubation for 24 h, the samples and 3.5 mM $CaCl_2$ as a differentiation-inducing control were combined for 5 days. Cell lysate was heated to 95 °C for 15 min, centrifuged at 20000 rpm for 60 min, and then analyzed at 430 nm. Total protein was determined using the Bradford assay.

3.7. PPAR-α binding assay

LanthascreenTM TR-FRET-based competitive binding assay kits (Invitrogen, MA, USA) were used to evaluate the PPAR-α binding activity of ligands according to the manufacturer's instructions. All assay measurements were performed using an Infinite 200 (Tecan, Mannedorf, Switzerland). WY14643 was used as the positive control.

3.8. Docking study

A possible binding model between PPAR-α and flavonols were predicted using docking simulations based on the complex structures of PPAR-α and its activator. The possible binding of three flavonols (kaempferol 3-glucoside, quercetin 3-glucoside, isorhamnetin 3-glucoside) were defined, and the known interactions between PPAR-α and the activator were considered. The binding sites of flavonols were expected to be similar to that of known PPAR-α ligands, and two recently reported PDB structures (7E5I. pdb and 7E5H.pdb) were used as references for the docking studies. The initial binding model was determined by a rigid docking study, and molecular mechanics energies combined with the generalized born and surface area (MM-GBSA) was used for final binding model prediction. The binding free energy is important parameter of MM-GBSA and is used to determine the binding affinity of drugs to target protein. MAESTRO (Schrödinger LLC, NY, USA) was used for all calculations using the Glide and Prime modules in a Linux environment with default parameters [14].

3.9. Measurement of intracellular reactive oxygen species

Intracellular reactive oxygen species (ROS) were determined using 2',7'-dichlorofluorescein diacetate (DCF-DA). RAW 264.7 cells were treated in the presence of 2 μg/mL lipopolysaccharide (LPS) together with samples at 37 ℃ for 1 h.

3.10. Measurement of nitric oxide, IL-6 and TNF-α production

Nitric oxide (NO) production in the medium was determined by reacting the sample with the Griess reagent. After RAW 264.7 cells were seeded in a 96-well plate at a concentration of 2.0 × 105 cells/well and incubated for 24 h in a 5% CO2 atmosphere and 37 ℃, they were stimulated with

 doi:10.20944/preprints202311.1891.v1

various concentrations of samples and 2 μg/mL LPS for 24 h. L-NMMA, a NO synthase inhibitor, was used as a positive control. IL-6 and TNF-α was determined using ELISA kit (R&D systems).

3.11. Reverse transcription-polymerase chain reaction (RT-PCR)

Total RNA was isolated from RAW 264.7 using the RNeasy Mini Kit (Qiagen, Netherlands). cDNA was synthesized by RT-PCR using a OneStep RT-PCR Kit (Qiagen, Netherlands). The mRNA levels of iNOS and β-actin (housekeeping gene) were measured by PCR with primers (Bioneer, Daejeon, Korea). The PCR conditions for each gene were as follows: mouse β-actin, 5'-TGGAATCCTGTGGCATCCATGAAAC-3' and 5'-TAAAACGCAGCTCAGTAACAGTCCG-3'; mouse iNOS, 5'-AGCCCAACAATACAAGATGACCCT-3' and 5'-TTCCTGTTGTTTCTATTTCCTTTGT-3'. The amplification profile consisted of denaturation at 94 °C for 1 min and annealing at 60 °C for 1 min.

3.12. Analysis of flavonols

Each fraction of the *E. sativa* was analyzed by HPLC-UV-MS. Approximately, 0.05 g of each fraction was weighed and ultrasonically extracted with 25 mL of methanol for 30 min. Then the extract was filtered through 0.45 μm membrane filter prior to analysis. The identification of flavonols was conducted on the HPLC-UV-MS system (Ultimate3000 UPLC system with PDA detector and LTQ-XL ion trap mass spectrometer, Thermo-Fisher Scientific). The chromatographic separation was performed on the analytical column (Hypersil GOLD, 2.1 × 200 mm, 1.9 μm) maintained at 35 ℃ and by the gradient elution of the mobile phase consisted of 100 mM formic acid in deionized water (mobile phase A) and acetonitrile (mobile phase B) at the flow rate of 0.2 mL/min. The gradient program was: from 0 (15% B) to 45 min (40% B); from 75 to 84 min (98% B); 85 to 90 min (15% B). Mass spectrometry with an electrospray ionization (ESI) source was conducted in the negative ion mode. The analysis was performed using full scan mode and data dependent MS2 in the mass range of m/z 50-1000. The MS settings were as follows: spray voltage, 5.0 kV; sheath gas, 30 Arb; auxiliary gas, 7 Arb; capillary temperature, 275 ℃; collision energy of MS2, 35%. The data were gathered using Xcaliver and Chromeleon software (Thermo-Fisher Scientific). Quantitative analysis was done by UV detection at 371 nm using appropriate standard reagents.

3.13. Statistical analysis

All data are presented as mean ± standard deviation (SD). Statistical analyses were performed using GraphPad Prism 5.0 (GraphPad Software, CA, USA). Comparisons between multiple groups were performed using one-way analysis of variance with Bonferroni's comparison of all pairs of columns. Statistical significance was set at $p < 0.05$.

5. Conclusions

Ethyl acetate fraction of *E. sativa* was analyzed to contain high amounts of three flavonols including kaempferol, quercetin, and isorhamnetin, and their mono-glycosides, which showed the best antioxidant, skin barrier function improvement via PPAR-α activation, and anti-inflammatory effects. In addition, three mono-glycoside flavonols such as kaempferol-3-glucoside, quercetin-3-glucoside and isorhamnetin-3-glucoside were demonstrated to be PPAR-α activators by molecular docking simulation. Taken together, these results suggest that *E. sativa* can be used as a therapeutic agent for maintaining healthy skin by alleviating inflammatory skin diseases such as atopic dermatitis.

Author Contributions: For research articles with several authors, a short paragraph specifying their individual contributions must be provided. The following statements should be used "Conceptualization, B.K. and W.C.; methodology, J.P.; software, J.Y.L.; validation, J.K.; formal analysis, W.C.; investigation, B.K.; resources, B.K.; data curation, H.W.K., B.K.; writing—original draft preparation, J.P.; writing—review and editing, W.C., B.K.; visualization, J.Y.L.; supervision, J.L.; funding acquisition, B.K. All authors have read and agreed to the published version of the manuscript.".

Funding: This work was supported by the National Research Foundation of Korea(NRF) grant funded by the Korea government(MSIT) (No. 2020R1A2C1005993).

Conflicts of Interest: The authors declare no conflict of interest.

References

1. Haftek, M.; Roy, D.C.; Liao, I.C. ARTICLE: Evolution of Skin Barrier Science for Healthy and Compromised Skin. J Drugs Dermatol 2021, 20, s3-s9.
2. Murata, T.; Honda, T.; Mostafa, A.; Kabashima, K. Stratum corneum as polymer sheet: concept and cornification processes. Trends Mol Med 2022, 28, 350–359.
3. Luger, T.; Amagai, M.; Dreno, B.; Dagnelie, M.A.; Liao, W.; Kabashima, K.; Schikowski, T.; Proksch, E.; Elias, P.M.; Simon, M.; Simpson, E.; Grinich, E.; Schmuth, M. Atopic dermatitis: Role of the skin barrier, environment, microbiome, and therapeutic agents. J Dermatol Sci 2021, 102, 142–157.
4. Furue, K.; Mitoma, C.; Tsuji, G.; Furue, M. Protective role of peroxisome proliferator-activated receptor α agonists in skin barrier and inflammation. Immunobiology 2018, 223, 327–330.
5. Hanley, K.; Jiang, Y.; Crumrine, D.; Bass, N.M.; Appel, R.; Elias, P.M.; Williams, M.L.; Feingold, K.R. Activators of the nuclear hormone receptors PPARalpha and FXR accelerate the development of the fetal epidermal permeability barrier. J Clin Invest 1997, 100, 705–712.
6. Wallmeyer, L.; Lehnen, D.; Eger, N.; Sochorová, M.; Opálka, L.; Kováčik, A.; Vávrová, K.; Hedtrich, S. Stimulation of PPARα normalizes the skin lipid ratio and improves the skin barrier of normal and filaggrin deficient reconstructed skin. J Dermatol Sci 2015, 80, 102–110.
7. Mao-Qiang, M.; Fowler, A.J.; Schmuth, M.; Lau, P.; Chang, S.; Brown, B.E.; Moser, A.H.; Michalik, L.; Desvergne, B.; Wahli, W.; Li, M.; Metzger, D.; Chambon, P.H.; Elias, P.M.; Feingold, K.R. Peroxisome-proliferator-activated receptor (PPAR)-gamma activation stimulates keratinocyte differentiation. J Invest Dermatol 2004, 123, 305–312.
8. Kim, B.; Choi, Y.E.; Kim, H.S. Eruca sativa and its flavonoid components, quercetin and isorhamnetin, improve skin barrier function by activation of peroxisome proliferator-activated receptor (PPAR)-α and suppression of inflammatory cytokines. Phytother Res 2014, 28, 1359–1366.
9. Bell, L.; Wagstaff, C. Glucosinolates, myrosinase hydrolysis products, and flavonols found in rocket (Eruca sativa and Diplotaxis tenuifolia). J Agric Food Chem 2014, 62, 4481–4492.
10. Yehuda, H.; Khatib, S.; Sussan, I.; Musa, R.; Vaya, J.; Tamir, S. Potential skin antiinflammatory effects of 4-methylthiobutylisothiocyanate (MTBI) isolated from rocket (Eruca sativa) seeds. Biofactors 2009, 35, 295–305.
11. Awadelkareem, A.M.; Al-Shammari, E.; Elkhalifa, A.O.; Adnan, M.; Siddiqui, A.J.; Mahmood, D.; Azad, Z.R.A.A.; Patel, M.; Mehmood, K.; Danciu, C.; Ashraf, S.A. Anti-Adhesion and Antibiofilm Activity of Eruca sativa Miller Extract Targeting Cell Adhesion Proteins of Food-Borne Bacteria as a Potential Mechanism: Combined In Vitro-In Silico Approach. Plants (Basel) 2022, 11, 610. doi: 10.3390/plants11050610.
12. Awadelkareem, A.M.; Al-Shammari, E.; Elkhalifa, A.E.O.; Adnan, M.; Siddiqui, A.J.; Snoussi, M.; Khan, M.I.; Azad, Z.R.A.A.; Patel, M.; Ashraf, S.A. Phytochemical and In Silico ADME/Tox Analysis of Eruca sativa Extract with Antioxidant, Antibacterial and Anticancer Potential against Caco-2 and HCT-116 Colorectal Carcinoma Cell Lines. Molecules 2022, 27, 1409. doi: 10.3390/molecules27041409.
13. Ikram, J.; Alamgeer, -.; Muhammad Irfan, H.; Akram, M.; Hussain Asim, M.; Hadal Alotaibi, N.; Saad Alharbi, K.; Abbas Bukhari, S.N.; Qasim, S.; Niazi, Z.R. Ethyl-acetate extract of tara mira (Eruca sativa) alleviates the inflammation and rheumatoid arthritis in rats. Pak J Pharm Sci 2021, 34, 1897–1902.
14. Lionta, E.; Spyrou, G.; Vassilatis, D.K.; Cournia, Z. Structure-based virtual screening for drug discovery: principles, applications and recent advances. Curr Top Med Chem 2014, 14, 1923–1938.
15. Swallah, M.S.; Sun, H.; Affoh, R.; Fu, H.; Yu, H. Antioxidant Potential Overviews of Secondary Metabolites (Polyphenols) in Fruits. Int J Food Sci 2020, 2020, 9081686.
16. Ullah, A.; Munir, S.; Badshah, S.L.; Khan, N.; Ghani, L.; Poulson, B.G.; Emwas, A.; Jaremko, M. Important Flavonoids and Their Role as a Therapeutic Agent. Molecules 2020, 25, 5243. doi: 10.3390/molecules25225243.
17. Dubrac, S.; Schmuth, M. PPAR-alpha in cutaneous inflammation. Dermatoendocrinol 2011, 3, 23–26.
18. Shin, M.H.; Lee, S.R.; Kim, M.K.; Shin, C.Y.; Lee, D.H.; Chung, J.H. Activation of Peroxisome Proliferator-Activated Receptor Alpha Improves Aged and UV-Irradiated Skin by Catalase Induction. PLoS One 2016, 11, e0162628.
19. Zhou, L.L.; Lin, Z.X.; Fung, K.P.; Che, C.T.; Zhao, M.; Cheng, C.H.; Zuo, Z. Ethyl acetate fraction of Radix rubiae inhibits cell growth and promotes terminal differentiation in cultured human keratinocytes. J Ethnopharmacol 2012, 142, 241–247.

20. Micallef, L.; Belaubre, F.; Pinon, A.; Jayat-Vignoles, C.; Delage, C.; Charveron, M.; Simon, A. Effects of extracellular calcium on the growth-differentiation switch in immortalized keratinocyte HaCaT cells compared with normal human keratinocytes. Exp Dermatol 2009, 18, 143–151.
21. Kim, S.O.; Han, Y.; Ahn, S.; An, S.; Shin, J.C.; Choi, H.; Kim, H.J.; Park, N.H.; Kim, Y.J.; Jin, S.H.; Rho, H.S.; Noh, M. Kojyl cinnamate esters are peroxisome proliferator-activated receptor α/γ dual agonists. Bioorg Med Chem 2018, 26, 5654–5663.
22. Zhang, X.; Perez-Sanchez, H.; Lightstone, F.C. A Comprehensive Docking and MM/GBSA Rescoring Study of Ligand Recognition upon Binding Antithrombin. Curr Top Med Chem 2017, 17, 1631–1639.
23. Genheden, S.; Ryde, U. The MM/PBSA and MM/GBSA methods to estimate ligand-binding affinities. Expert Opin Drug Discov 2015, 10, 449–461.
24. Chen, D.; Oezguen, N.; Urvil, P.; Ferguson, C.; Dann, S.M.; Savidge, T.C. Regulation of protein-ligand binding affinity by hydrogen bond pairing. Sci Adv 2016, 2, e1501240.
25. Bell, L.; Oruna-Concha, M.J.; Wagstaff, C. Identification and quantification of glucosinolate and flavonol compounds in rocket salad (Eruca sativa, Eruca vesicaria and Diplotaxis tenuifolia) by LC-MS: highlighting the potential for improving nutritional value of rocket crops. Food Chem 2015, 172, 852–861.
26. Bennett, R.N.; Rosa, E.A.S.; Mellon, F.A.; Kroon, P.A. Ontogenic profiling of glucosinolates, flavonoids, and other secondary metabolites in Eruca sativa (salad rocket), Diplotaxis erucoides (wall rocket), Diplotaxis tenuifolia (wild rocket), and Bunias orientalis (Turkish rocket). J Agric Food Chem 2006, 54, 4005–4015.
27. Dall'Acqua, S.; Ertani, A.; Pilon-Smits, E.A.H.; Fabrega-Prats, M.; Schiavon, M. Selenium Biofortification Differentially Affects Sulfur Metabolism and Accumulation of Phytochemicals in Two Rocket Species (Eruca Sativa Mill. and Diplotaxis Tenuifolia) Grown in Hydroponics. Plants (Basel) 2019, 8, 68. doi: 10.3390/plants8030068.
28. Cuellar, M.; Baroni, V.; Pfaffen, V.; Griboff, J.; Ortiz, P.; Monferrán, M.V. Uptake and accumulation of Cr in edible parts of Eruca sativa from irrigation water. Effects on polyphenol profile and antioxidant capacity. Heliyon 2021, 7, e06086.